Structure and Biosynthesis of Amphidinol 17, a Hemolytic Compound from *Amphidinium carterae*[⊥]

Yanhui Meng, Ryan M. Van Wagoner, Ian Misner, Carmelo Tomas, and Jeffrey L. C. Wright*

Center for Marine Science, University of North Carolina Wilmington, 5600 Marvin Moss Lane, Wilmington, North Carolina 28409

Received October 5, 2009

Amphidinol 17 (AM17; **1**), a novel amphidinol, has been isolated from a Bahamas strain of *Amphidinium carterae*. This new congener contains the signature hairpin region and a Δ^6 polyene arm, whereas the polyol arm is distinct from those of other amphidinols. The pattern of acetate incorporation in **1** was directly determined by feeding a single labeled substrate, [2-^{13}C]acetate. While the highly conserved regions within the amphidinol family of AM17 have exhibited identical occurrences of cleaved acetates to other amphidinols for which the biosynthesis has been explored, the polyol arm for AM17 displays a higher degree of nascent chain processing that shows similarities to amphidinolide biosynthesis. AM17 exhibited an EC_{50} of 4.9 μM in a hemolytic assay using human red blood cells but displayed no detectable antifungal activity.

Dinoflagellates of the genus *Amphidinium* Claparéde & Lachmann belong to the order Gymnodiniales and the family Gymnodiniaceae.[1] Early reports of hemolytic, ichthyotoxic, and antifungal activities from extracts of *Amphidinium carterae* Hulbert led to the isolation and identification of amphidinol 1.[2] Since then, nearly 20 closely related toxins known collectively as the amphidinols (AMs) have been isolated from various marine dinoflagellates belonging to the genus *Amphidinium*.[3−6] Other related analogues have been reported such as the luteophanols,[7] lingshuiol,[8] and karatungiol,[9] displaying cytotoxic and antifungal activity, respectively, and carteraol E, an ichthyotoxin from another clone of *A. carterae*.[10] More recently, the structure of a closely related compound called karlotoxin that belongs to a group of fish-killing toxins produced by *Karlodinium veneficum* was described,[11] and this was the first report of such a compound from a dinoflagellate other than *Amphidinium*. In general terms, all members of this group of natural products are characterized by a long polyhydroxy chain, together with a polyene chain connected by an intermediate C_{16} section containing two pyran rings separated by a short C_6 aliphatic chain. The latter portion of the molecule is largely invariant among the different amphidinols, with most structural variety resulting from differences in the length and substitution pattern of the polyol portion ($C_{23}-C_{37}$) and from variations in the length ($C_{16}-C_{18}$) and degree of unsaturation of the polyene section ($\Delta^2-\Delta^6$). The potent antifungal activity displayed by various members of the family, which exceeds that of commercial antifungal compounds such as amphotericin B, has prompted interest in their mechanism of action, which is believed to be different from that of amphotericin B.

We report here the isolation and structure determination of amphidinol 17 (AM17; **1**) from *A. carterae*. Unusual features of the polyol arm of AM17 suggested that characterizing the pattern of acetate incorporation would help delineate the biosynthesis of this family of compounds. Following consideration of the original labeling study, coupled with our current knowledge of dinoflagellate biosynthesis, we reasoned that by using an optimal precursor it would be possible to unravel the biogenesis of AM17 in a single labeling experiment. Given the large culture volumes necessary to obtain a few milligrams of material for analysis, such an approach would also save considerable time and cost of ^{13}C-labeled precursors. This paper describes the structure elucidation of AM17 (**1**) and its biogenesis as revealed by using only [2-^{13}C]acetate as a precursor.

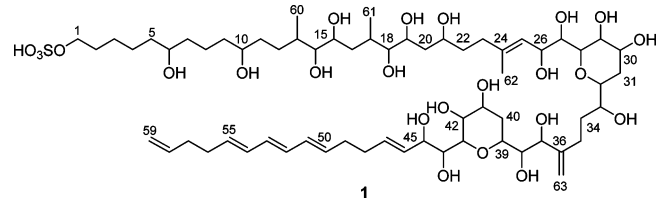

1

Results and Discussion

Extracts from both the harvested *A. caterae* cells and medium were partitioned between MeOH and hexanes. The MeOH layer was dried and partitioned between *n*-BuOH and water to yield an amphidinol-rich *n*-BuOH phase. The *n*-BuOH phase was dried and subjected to a series of chromatographic steps to afford a novel sulfated amphidinol derivative, AM17 (**1**; Figure 1) as a pale yellow semisolid. The high-resolution mass spectrometric data suggested a molecular formula of $C_{63}H_{110}O_{24}S$, while the UV maxima at 262, 272, and 283 nm suggested the presence of a conjugated triene chromophore. The NMR data (Table 1) in MeOH-d_4 revealed a total of 63 carbon signals, which were assigned to two quaternary sp^2 carbons, 10 sp^2 methines, two sp^2 methylenes, 24 sp^3 methines (of which 22 were oxygenated), 22 sp^3 methylenes, and three methyls. A total of nine degrees of unsaturation were accounted for by seven double bonds and two rings. All these data suggested that **1** is an amphidinol homologue. The occurrence of *m*/*z* 79 and 97 as products of *m*/*z* 1281 ($[M - H]^-$) by negative-ion MS/MS indicated the presence of a sulfate ester in **1**. Detailed analysis of the COSY, TOCSY, HSQC, and HMBC spectra of **1** (Table 1) led to assignments of the following three partial structures: A (from C-1 to C-23), B (from C-25 to C-35), and C (from C-37 to C-59) (Figure 2). For partial structure A, the COSY and TOCSY data revealed connectivities of H-1−H-3, H-5−H-7, and H-9−H-23. The two doublet methyl groups (H_3-60 and H_3-61) exhibited COSY correlations to H-13 and H-17, respectively. Connectivities from C-3 to C-5 and from C-7 to C-9 were established through HMBC correlations from H-2 and H-3 to C-4, from H-5 to C-3, and from H-7 and H-9 to C-8. An oxygenated methylene assigned to C-1 displayed low-field proton and carbon chemical shifts (δ_H 3.90 and δ_C 69.25), consistent with this as the site of attachment for the sulfate group. This was confirmed further by comparing the carbon chemical shifts of C-1−C-3 with those in lingshuiol B, a known

[⊥] Dedicated to the late Dr. John W. Daly of NIDDK, NIH, Bethesda, Maryland, and to the late Dr. Richard E. Moore of the University of Hawaii at Manoa for their pioneering work on bioactive natural products.

* To whom correspondence should be addressed. Tel: 910-962-2397. Fax: 910-962-2410. E-mail: wrightj@uncw.edu.

10.1021/np900616q
Published on Web 01/28/2010

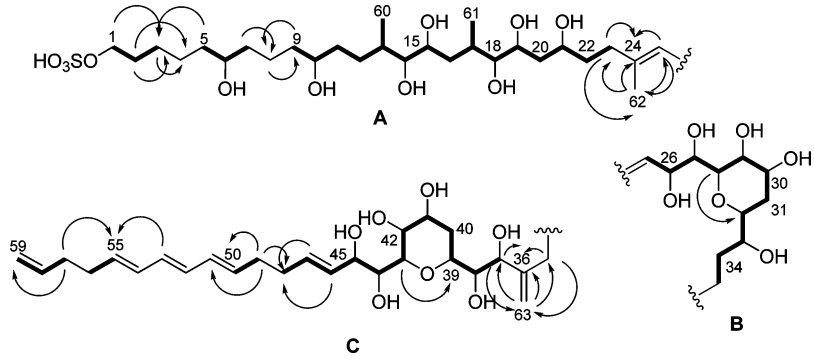

Figure 1. Important NMR correlations in the elucidation of three partial structures (A, B, and C) in **1**. Bold bonds indicate COSY/TOCSY correlations. Arrows indicate key HMBC correlations.

amphidinol that has a similar sulfated ester link at C-1 of the polyol side chain.[4,8] In partial structure B, the connectivities from H-25 to H-35 were easily determined by the cross-peaks observed in the COSY and TOCSY spectra. The link between C-28 and C-32 through an oxygen to form a tetrahydropyran ring was determined by the HMBC correlation between H-28 (δ_H 3.88) and C-32 (δ_C 75.79). For partial structure C, the overlapped signals of H-51, H-52, H-53, and H-54 were correlated with H-50 and H-55 in the COSY spectrum, and the UV maxima at 262, 272, and 283 nm suggested that C-50 through C-55 formed a conjugated triene group, a feature common in this class of compounds. The geometry of the $\Delta^{46,47}$ isolated double bond was assigned as *E* on the basis of the coupling value ($^3J_{H-H}$ = 14.8 Hz) between the olefinic protons. This double bond was separated from the triene system by two methylene groups, C-48 and C-49, as determined by COSY cross-peaks H-46/H-47 and H-49/H-50, and by a series of HMBC correlation peaks from H-49 to C-50 and C-48 and from H-46, H-47, and H-49 to C-48. The terminal vinyl group at C-58 was also linked to the triene system through two methylenes, as revealed by the COSY cross-peaks H-58/H-59 and H-55/H-56 and the HMBC correlation peaks from H-53 and H-57 to C-55 and from H-57 to C-59. The connectivities from H-37 to H-46 in substructure C were established primarily using COSY data. The presence of the tetrahydropyran ring from C-39 to C-43 was indicated by a HMBC correlation from H-43 to C-39. The ^{1}H and ^{13}C NMR data (Table 1) from C-48 to C-59 agreed well with those from C-44 to C-52 of amphidinol 7 (AM7),[6] which suggested that the geometries of the double bonds in the triene are all *E*, but the severe signal overlap prevented any additional NMR analysis.

Finally, the partial structures A, B, and C were linked together on the basis of key HMBC correlations. The connection of substructure A and B through a quaternary sp^2 carbon (C-24, δ_C 139.4) bearing a vinylic methyl group (H_3-62, δ_H 1.67) was determined by HMBC correlations from H_3-62 to C-23, C-24, and C-25 and from H-23 and H-25 to C-24 and C-62. The geometry of the $\Delta^{25,26}$ double bond was assigned as *E* on the basis of the characteristic carbon chemical shift of C-62 (δ_C 17.4).[4,10] Substructure B was linked to C through an sp^2 quaternary carbon (C-36, δ_C 151.49), which formed a double bond with a vinylic methylene (C-63, δ_C 113.34), as determined by a series of HMBC correlations from H-63 to C-35, C-36, and C-37 and from H-35 and H-37 to C-36 and C-63. Thus, the structure of **1** was determined as a new sulfated amphidinol congener. Further confirmation of the structure of AM17 was obtained from mass spectral fragmentation. The negative-ion enhanced product ion spectrum for *m/z* 1281.5 ([M − H]$^-$) provided a wealth of structural information by charge-remote fragmentation due to the presence of the sulfate group.[6] The fragmentation pattern of **1** corresponded with the proposed arrangement of substituents and functional groups in the molecule, and indeed all the fragment ions could be assigned (Figure 2).

AM17 (**1**) was tested for its hemolytic potency against human red blood cells and for its antifungal activity against the fungi *Aspergillus niger* and *Candida kefyr*. For the hemolytic assay, an EC_{50} of 4.9 μM was obtained. This level of potency is relatively weak within the amphidinols, which have been reported to have EC_{50} values as low as the low to mid nanomolar range.[11,12] However, AM17 (**1**) is comparable in this respect to other sulfated amphidinols, which tend to be weaker by roughly 5- to 10-fold than their nonsulfated congeners.[4] AM17 did not produce detectable antifungal activity, which also appears to be negatively impacted by sulfation.[4]

AM17 (**1**) described here is different from other amphidinols in that it contains a polyol chain of intermediate length (C_{27}) with a unique arrangement of substituents including a terminal sulfate group and an extremely hydrophobic polyene chain (C_{16}; Δ^6). The amphidinols are known to increase membrane permeability, and in vitro studies have shown this effect can be potentiated by lipid constituents such as sterols[13] and glycophorin A,[14] a major membrane integral protein of erythrocytes. A structure−activity study of several amphidinol derivatives[6] showed that the hydrophobicity of the polyene chain is critical for activity and that the polyol chain, regardless of chain length, appears to have only a moderate effect on potency, aside from the aforementioned decrease in potency due to sulfation.

Biosynthetic studies of dinoflagellate metabolites have been limited to just a few compounds: two brevetoxin derivatives,[15,16] several DSP compounds,[17−20] amphidinols,[21] goniodomin,[22] amphidinolides,[23] and a spirolide.[24] Thus, it was of interest to examine the biosynthesis of this new amphidinol derivative. In general, the limited number of biosynthetic experiments with dinoflagellates is a consequence of several factors including the difficulty in obtaining efficient incorporation of precursors with no scrambling of the label and the very low yield of metabolites that are produced by such cultures, which necessitates large culture volumes. Despite these limitations, a previous study by Murata's group established the polyketide origin of two amphidinols, AM2 and AM4.[21] The biosynthetic pathway was characterized by many of the assembly features characteristic of dinoflagellate polyketide biogenesis, namely, the deletion of carboxyl carbon atoms of intact acetate units from the nascent polyketide chain[18,20] and the addition of pendant methyl groups derived from the methyl group of acetate,[15,16,18,20] rather than *S*-adenosyl methionine (SAM), the more common methylating agent in polyketides. These complexities in the pathway, which are entirely unpredictable and cannot be reliably interpreted by a "paper biogenetic" analysis, necessitate isotope labeling experiments in order to establish the true biosynthetic pathway. Curiously, it is this very complexity in the biogenesis of these molecules that permits the possibility of unraveling the biosynthetic pathway in a single labeling experiment. In this case, such an approach was considered extremely attractive in that it would save considerable time by avoiding the necessity of conduct-

Table 1. ^{1}H NMR, ^{13}C NMR, and HMBC Data of Compound **1** in MeOH-d_4[a]

posn.	δ_C, mult.[b]	^{13}C label state[c]	δ_H, mult, J_{H-H} (Hz)	HMBC[d]
1	69.25, CH_2	*	3.90, t (6.7)	H-2
2	30.61, CH_2	*	1.59, m	H-1, H-4
3	27.18, CH_2	**	1.33, m	H-1, H-4, H-5
4	26.61, CH_2	*	1.30, m	H-2, H-3
5	38.61, CH_2	**	1.42, m; 1.30, m	H-7a, H-8a
6	72.63, CH	*	3.46, m	H-5a, H-5b, H-7a, H-7b
7	38.65, CH_2	**	1.42, m; 1.30, m	H-8a, H-8b
8	23.09, CH_2	*	1.51, m; 1.30, m	H-7a, H-7b, H-9a, H-9b
9	38.50, CH_2	**	1.43, m; 1.30, m	H-8a, H-8b
10	73.24, CH	*	3.43, m	H-9b, H-11b
11	35.91, CH_2	**	1.49, m; 1.25, m	H-9a, H-12b, H_3-60
12	29.11, CH_2	*	1.68, m; 1.07, m	H-14, H_3-60
13	36.94, CH	***	1.60, m	H-12b, H_3-60
14	80.26, CH	***	3.01, dd (7.1, 3.7)	H-12a, H_3-60
15	70.30, CH	***	3.66, m	H-16a, H-17
16	39.96, CH_2	*	1.50, m; 1.29, m	H_3-61
17	31.57, CH_2	***	2.01, m	H-16a, H-16b, H-18 (w), H_3-61
18	79.80, CH	***	3.18, dd (7.9, 3.4)	H-19, H_3-61
19	72.48, CH	*[e]	3.60, m	H-17, H-18, H-20b
20	41.40, CH_2	**	1.88, m; 1.44, m	H-18, H-19
21	71.73, CH	*	3.78, m	H-20b, H22a, H-23a (w), H-23b (w)
22	36.65, CH_2	**	1.60, m; 1.50, m	H-23a (w), H-23b (w), H_3-62
23	36.85, CH_2	*	2.12, m; 2.05, m	H-25, H_3-62
24	139.4, qC	***		H-23a, H-23b, H-25, H-26, H_3-62
25	126.4, CH	***	5.40, d (8.9)	H-23a, H-23b, H-26, H-27 (w), H_3-62
26	68.04, CH	*	4.45, dd (8.9, 2.4)	H-25, H-27, H-28
27	72.48, CH	**	3.60, m	H-25, H-28
28	79.33, CH	*	3.88, m	H-26 (w), H-27
29	68.86, CH	**	3.95, m	H-27, H-31
30	67.52, CH	*	3.89, m	H-28, H-31
31	30.47, CH_2	**	1.70, m	H-29. H-30
32	75.79, CH	*	3.41, m	H-28, H-30, H-31
33	74.45, CH	**	3.52, m	H-34b (w), H-35b (w)
34	32.56, CH_2	*	1.88, m; 1.49, m	
35	28.10, CH_2	**	2.33, m; 2.03, m	H-37, H-63a, H-63b
36	151.49, qC	*		H-35a, H-35b, H-37, H-38, H-63a, H-63b
37	76.79, CH	**	4.10, d (9.5)	H-38, H-39, H-63a, H-63b
38	75.27, CH	*	3.26, m	H-37
39	70.60, CH	***	3.96, m	H-37, H-40a, H-43
40	31.60, CH_2	***	2.01, m; 1.48, m	H-38, H-41
41	67.42, CH	*	3.94, m	H-39, H-43
42	68.99, CH	**	3.95, m	
43	80.67, CH	*	3.66, m	H-44
44	72.01, CH	**	3.89, m	H-43
45	74.26, CH	*	4.28, d (8.4)	H-44, H-46, H-47
46	129.21, CH	***	5.55, dd (14.8, 8.4)	H-44, H-45, H-47 (w), H-48 (w)
47	135.21, CH	***	5.71, m	H-45, H-46, H-48
48	33.50, CH_2	*	2.10, m	H-46, H-47, H-49
49	33.80, CH_2	**	2.10, m	H-48, H-50, H-51
50	134.7, CH	*	5.60, m	H-49, H-51, H-52
51	132.5, CH	—[f]	5.98, m	H-49, H-53
52	132.3, CH	—[f]	5.98, m	H-50, H-54
53	132.4, CH	—[f]	5.98, m	H-55
54	132.5, CH	—[f]	5.98, m	H-52, H-56
55	134.5, CH	**	5.65, m	H-53, H-57
56	33.90, CH_2	*	2.10, m	H-54, H-58
57	34.90, CH_2	**	2.07, m	H-59a, H-59b
58	139.50, CH	*	5.73, m	H-56
59	115.50, CH_2	**	4.93, m; 4.87, m	H-57
60	17.01, CH_3	***	0.87, d (6.9)	H-12a, H-12b, H-13, H-14
61	13.21, CH_3	***	0.86, d (7.2)	H-16a, H-16b, H-17
62	17.41, CH_3	***	1.67, s	H-23a, H-23b, H-25
63	113.34, CH_2	**	4.99, s; 4.90, s	H-35a, H-37

[a] Chemical shifts referenced to residual solvent signals at 3.30 and 49.0 ppm for ^{1}H and ^{13}C, respectively. [b] As inferred by DEPT or phase-sensitive HSQC. [c] For material isolated from a culture incubated with [2-^{13}C]acetate. * = no enhancement, no satellites; ** = enhancement without satellites; *** = enhancement with satellites. States are as depicted in Figure 3. [d] *w* = weak cross-peak. [e] Deduced from lack of satellites for neighboring positions. [f] Not determined due to extensive spectral overlap.

ing several labeling experiments, as well as significant savings in the cost of labeled precursors given the extremely large culture volumes (>70 L) that are often required to produce sufficient material.

The crux of the approach was to supply [2-^{13}C]acetate as a precursor to cultures of *A. carterae* and monitor the nature of the signals associated with the labeled carbons in the enriched metabolite. We reasoned that several dinoflagellate-specific processes could occur, all of which could be identified by the resulting patterns of enrichment and ^{13}C−^{13}C coupling satellites. These possibilities are illustrated in Figure 3. The key phenomenon that enables this analysis is the occurrence of ^{13}C−^{13}C coupling between

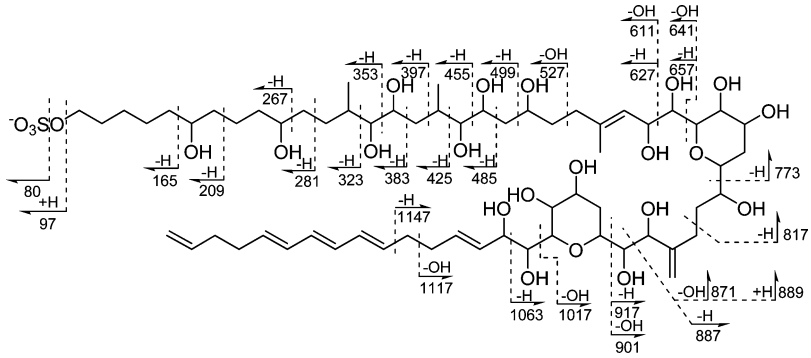

Figure 2. Proposed assignment of product ions of *m*/*z* 1281 by charge-remote fragmentation of **1**.

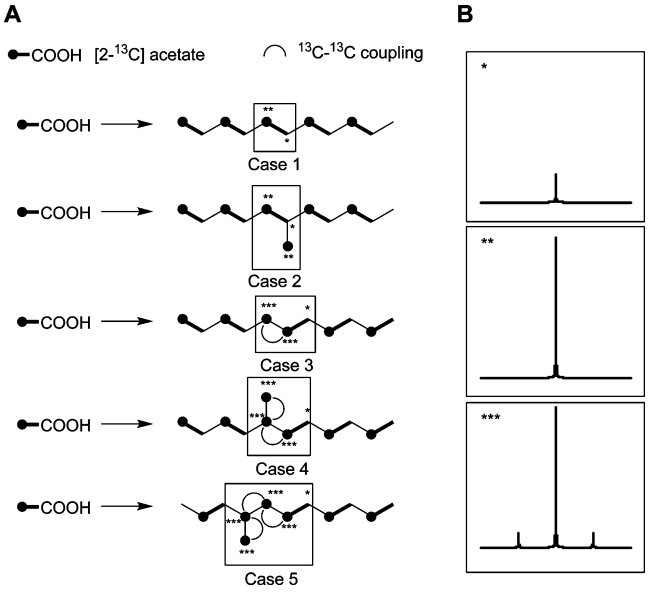

Figure 3. Theoretical labeling and $^{13}C-^{13}C$ coupling patterns in a dinoflagellate molecule following incorporation of [2-^{13}C]acetate. (A) Different labeling patterns in a polyketide chain as a result of carbon deletion steps and the addition of pendant alkyl groups from acetate. (B) The different types of ^{13}C NMR signals that would result as a consequence of labeling patterns shown in A and reported in Table 1.

adjacent labeled positions as a result of carbon deletion steps of the type that are frequently observed in dinoflagellates, as well as the introduction of pendant alkyl groups derived from the methyl carbon of acetate. Under the labeling regime employed in this study, three types of carbon resonances can be observed: * unenriched peaks with no coupling satellites; ** enriched peaks with no coupling satellites; and *** enriched peaks with coupling satellites. The patterns of occurrence of these three basic types allow one to draw inferences about the biosynthetic processes involved in compound production as described below.

In case 1, where only intact acetate units occur, the signal for a labeled carbon derived from [2-^{13}C]acetate would appear as an enriched singlet resonance in the ^{13}C NMR spectrum.

In case 2, a pendant methyl group derived from the methyl group of acetate, following Aldol condensation to a carbon derived from an acetate carboxyl of an intact acetate unit, would also appear as an enriched singlet.

In case 3, where an intact acetate unit has undergone deletion of the carboxyl-derived carbon, the resulting polyketide chain now contains two labeled carbons juxtaposed. When the level of enrichment is high enough that a significant population of labeled units also has labeled neighbors (typically ca. 2−3% above natural abundance),[25] the resultant J_{C-C} coupling would result in both labeled carbons displaying $^{13}C-^{13}C$ satellites straddling the natural abundance singlet resonance.

In case 4, a pendant methyl group is attached to a methyl-derived carbon in a deleted unit as described in case 3, resulting in three enriched contiguous carbons displaying satellites as a result of $^{13}C-^{13}C$ coupling. However, the highest possible multiplicity of signals as a result of the additional coupling is not observed because of the very low probability of three enriched carbons occurring together in the same individual molecule.[25] For example, if three adjacent carbons are theoretically enriched 10% above natural abundance (a significant enrichment level), the probability of all three adjacent carbons being present in the same labeled molecule is very low (i.e., $0.1 \times 0.1 \times 0.1 = 0.001$). The net result is that three adjacent enriched carbon atoms would only display $^{13}C-^{13}C$ doublets and would not show any additional coupling. In cases where the central carbon atom had significant differences in the $^1J_{C-C}$ values from its labeled atom neighbors (e.g., a methylated olefin), then both sets of satellites would be observed. In the labeling experiment with AM17 (**1**; Table 1), ^{13}C enrichment was on the order of ∼5% above natural abundance, an enrichment level that permits the observation of coupling satellites between adjacent labeled carbons, but which would preclude the observation of any higher-order coupling satellites. Moreover, all adjacent labeled atoms are connected to one another by σ-bonds with similar $^1J_{C-C}$ values; hence at most only one set of overlapped satellite peaks was observed for each resonance.

In case 5, the carboxyl carbons of two contiguous acetate units are deleted and a pendant methyl group is attached to the methyl-derived carbon of the second cleaved unit. Consequently, four adjacent enriched carbon atoms each display $^{13}C-^{13}C$ satellites. Note that if the pendant methyl group was attached to the methyl-derived carbon of the first cleaved acetate unit, the same result would be observed, namely, the appearance of four adjacent labeled carbons each displaying $^{13}C-^{13}C$ satellites, with no observable additional coupling.

The results obtained following incorporation of [2-^{13}C]acetate are included in Table 1. The enrichment patterns observed revealed that the carbon chain of AM17 (**1**) is derived entirely from acetate units, including the pendant carbon atoms. Both C-1 and C-2 of the chain were unlabeled, similar to a result obtained for AM4, and this portion of the chain is likely derived from a glycolate starter unit[21] as observed in okadaic acid and its analogues.[17] Most of the carbon resonances assigned to carbons of the polyketide chain that are derived from the methyl group of acetate appeared as enriched singlets. The exceptions were C-13, -14, -15, -17, -18, -24, -25, -39, -40, -46, and -47, which displayed resonances with $^{13}C-^{13}C$ satellites consistent with carbons derived from the methyl group of a cleaved acetate group (case 3). All the pendant alkyl groups were enriched, indicating they are derived from the methyl group of acetate, just as in the case of the okadaic acid family of compounds and esters.[19,20] Of these, only the exomethylene group (C-63) appeared as an enriched singlet in the ^{13}C NMR spectrum,

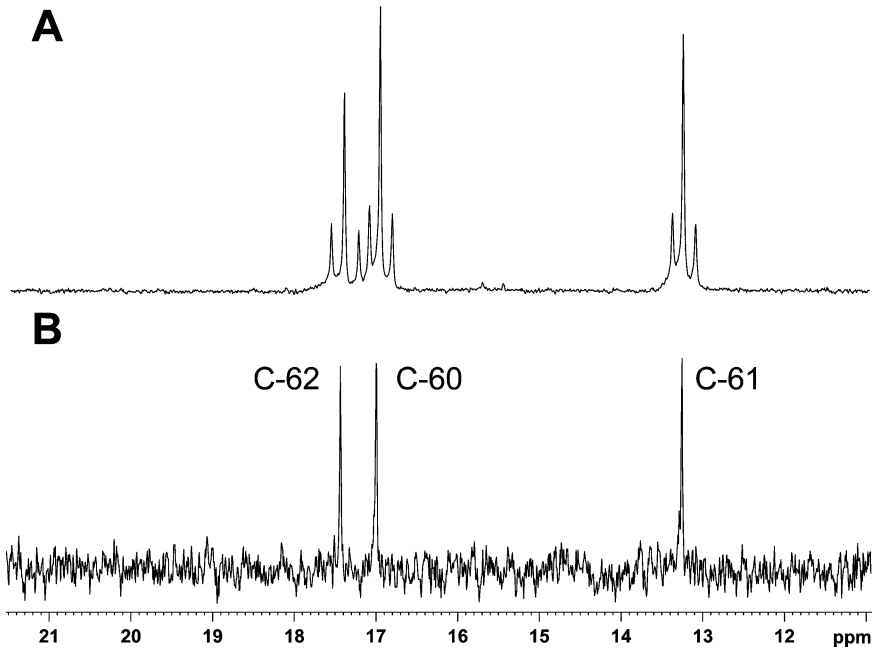

Figure 4. Comparison of the methyl signals from the ^{13}C NMR spectra of AM17. (A) [2-^{13}C]Acetate-labeled AM17. (B) Natural abundance AM17.

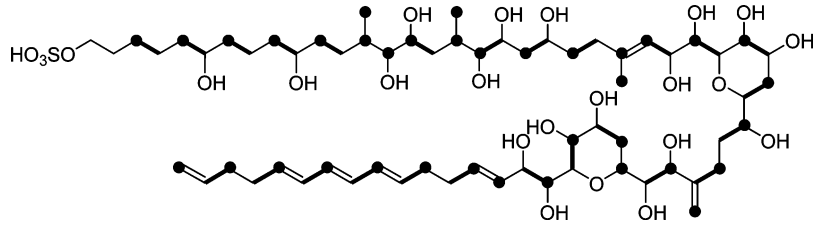

Figure 5. Proposed biosynthesis of AM17 as determined from the patterns of labeling and $^{13}C-^{13}C$ coupling satellites following incorporation of [2-^{13}C]acetate by *A. carterae*.

in line with attachment to a carboxyl-derived carbon of an acetate unit, as illustrated in case 2. The resonances for the remaining pendant methyl groups (C-60, -61, -62) were all enriched and all displayed $^{13}C-^{13}C$ satellites in the ^{13}C NMR spectrum (Figure 4), consistent with attachment to a methyl-derived carbon of a cleaved acetate group (case 4 and 5).

The biosynthetic labeling scheme for AM17 (**1**) is shown in Figure 5. Due to a high degree of spectral overlap for C-51−C-54, it was not possible to determine the exact labeling pattern for these carbons. However, the total peak areas suggest that two of the four carbons were enriched and there were no apparent satellite peaks for carbons C-51−C-55, implying intact incorporation of acetate without deletion at the positions in question. Consequently, it is possible to conclude that the labeling pattern observed for the hydrophobic polyunsaturated C_{16} chain (C-44 to C-59) in AM17 is identical with the pattern observed with AM2 and AM4. Both C-46 and C-59 are derived from a cleaved acetate unit, while the rest of this portion of the molecule is assembled from seven intact units. Similarly, the labeling pattern of the so-called "hairpin loop" region from C-26 through C-43 is also identical with AM2 and AM4, in which C-39 is the only carbon of a cleaved acetate unit, and the exomethylene carbon (C-63) arises from the methyl of an acetate unit by Aldol condensation with an electrophilic carboxyl carbon of an intact acetate unit (β-alkylation).

In contrast, the polyol region of AM17 shows much more variability compared with other amphidinols, not surprising in view of the fact that this is where most structural variety occurs among this group of metabolites. Although C-3−C-27 of the polyol section are all derived from acetate, there is a considerable degree of processing, and four acetate units are cleaved. In fact, three carbon deletion steps occur over a six-carbon stretch of this region (C-13−C-18), to yield a labeling pattern not unlike those found in some amphidinolides that similarly undergo high degrees of processing.[23] The three pendant methyl groups (C-60, -61, -62) arising in this region are all derived from acetate methyl, and each one is attached to the methyl of a cleaved acetate unit. This is in contrast to the results obtained with AM2, in which only two acetate units are cleaved and four of the five pendant methyl groups in this region are derived from acetate methyl but are attached to the carboxyl carbon of an intact acetate unit. While differences in the labeling pattern of the polyol region were expected, it was impossible to predict the labeling sequence that was observed. It appears that this part of the assembly process by the amphidinol polyketide synthase is highly variable, whereas the remainder of the biosynthetic process is remarkably stable and consistent. This may be related to the highly oxygenated nature of the polyol arm and the higher incidence of oxidation of methyl carbons in deleted acetate units, which also may be linked to the Favorskii oxidative rearrangement reactions.[19,26,27] The presence of more deletion steps in the polyol arm of AM17 (**1**) follows a general trend in dinoflagellate metabolites: The less the compounds look like typical (i.e., linear, unbranched) fatty acids or simple polyketides, the more extensive editing (carbon deletion) or processing of the putative polyketide chain has occurred. Such a correlation is not trivial however, given the success by other organisms such as actinomycetes and fungi in performing topologically similar modifications (alkylation, hydroxylation, ring formation) of the nascent polyketide without the intervention of chain editing.

In summary, the isolation of AM17 (**1**) from *A. carterae* adds yet another amphipathic molecule to the arsenal of such hemolytic

agents produced by this genus of dinoflagellate. In this case the molecule diverges from others in that the sulfate ester group is attached at C-1, while C-2, a more common site for sulfation among the amphidinols, is not even hydroxylated. Further comparison shows that the polyol side chain is of intermediate length (C_{27}) compared with other amphidinols, with the only unit of unsaturation occurring in the form of a double bond universally present in amphidinols (note: this double bond is not present in karlotoxin).[11] The labeling experiments using only a single labeled precursor were remarkably successful and simplified the data interpretation and considerably reduced the cost of such stable isotope labeling experiments. The very complexities of dinoflagellate biosynthesis, namely, deletion of a carboxyl carbon of an intact acetate unit and C-methylation by an Aldol condensation requiring another molecule of acetate, make it possible to quickly delineate the assembly of complex dinoflagellate polyketides.

Experimental Section

General Experimental Procedures. All solvents employed for chromatography were HPLC grade (Burdick & Jackson/Honeywell). Optical rotation data were recorded on a Randolph Research Analytical Autopol III automatic polarimeter. UV spectra were recorded on a Beckman DU 640 spectrophotometer. IR data were recorded on a Madison CYGNUS 100 infrared spectrometer coupled with Winfirst software. ^{1}H NMR, COSY, HSQC, and HMBC spectra were recorded in MeOH-d_4 using a 500 MHz Bruker NMR Avance spectrometer. LC/MS were recorded on a Hewlett-Packard 1100 HPLC system with diode array detector using a Waters XTerra MS C_{18} column (2.1 × 30 mm) and a gradient mobile phase of MeCN/H_2O (each containing 0.1% acetic acid). A Waters/Micromass ZQ detector equipped with an electrospray ionization source was used to acquire mass spectrometric data. The cone voltages were set up at 40 V for negative-ion mode and 30 V for positive-ion mode. The LC-MS data were analyzed using MassLynx 4.1. High-resolution mass spectra were obtained using an Applied Biosystems Q Star XL spectrometer. Enhanced product ion spectra of *m*/*z* 1281.6 were acquired in the negative-ion mode on an Applied Biosystems Q Trap linear ion trap quadrupole LC/MS/MS system by flow-injection analysis of a purified sample using an ion source potential of −4500 V, a declustering potential of −60 V, a collision energy of −122 eV, and a collisionally activated dissociation gas pressure parameter of high. HPLC analysis and preparation was conducted on a Waters 1525 HPLC coupled with a Waters 2487 dual λ absorbance UV detector. The UV wavelengths used for separations were 214 and 272 nm. The flow rate of the mobile phase was 2 mL/min for 10 mm columns and 1 mL/min for 4.66 mm columns. Diaion HP-20 solid-phase extraction of the spent culture medium was accomplished using a Büchi C-605 pump with a Büchi C-615 pump manager.

Hemolytic Assay. Human red blood cells were obtained from the American Red Cross. Erythrocytes were washed, centrifuged, and diluted to (4.2−4.7) × 10^4 cells/mL with ELA buffer.[28] The modified erythrocyte lysis assays were performed in 96-well V-bottom microtiter plates (Costar) using 125 μL of erythrocyte suspension and 125 μL of compound diluted with ELA buffer. Saponin from quillaja bark (20−35% sapogenin content; Sigma, Inc.) was used as a positive control. Samples at each concentration were tested in triplicate. Plates containing sample and erythrocytes were incubated in sealed plates at 4 °C for 24 h and centrifuged, and the supernatants analyzed for optical densities at 415 nm. EC_{50} values were determined using nonlinear regression analysis in GraphPad Prism.

Antifungal Assay. Antifungal activity was determined using a standard disk-diffusion assay. A solution of the test compound in MeOH was applied to a 6 mm diameter filter paper and air-dried. The disk was transferred to an agar plate overgrown with *Aspergillus niger* (ATCC 16404) or *Candida kefyr* (ATCC 2512), and the development of zones of growth inhibition was measured from the outer edge of the disk. Amphotericin B (Fisher Scientific) was used as a positive control.

Biological Material. The dinoflagellate *Amphidinium carterae*, clone CMSTAC 14001, was isolated from a sample collected in Little San Salvadore Island, Bahamas, in 2004. This culture is deposited and maintained in the Center for Marine Science Toxic Algal Culture Collection (curator C. Tomas). Single cells were pipet isolated from a raw sample and placed into dilute K medium[29] at a salinity of 39 and grown at 25 °C and a fluence rate of 50−60 mol photons m^{-2} s^{-1} of cool white fluorescent light. A photoperiod of 14:10 h light:dark was used for cultivation of large batches. Once established as a stable culture, this clone was maintained in 250 mL Erlenmeyer flasks with monthly transfers. For experimental studies, *A. carterae* were grown in multiple 10 L batch cultures and harvested as a pellet using a Kendro continuous flow head and a Sorvall RC2-B refrigerated centrifuge. Once processed, the pellet of approximately 100 L was removed from the collection tubes as a moist pellet and stored in 15 mL cryovials at −80 °C until extraction and processing. Clear supernatant was collected in a 45 L glass aspirator bottle and processed as below for supernatant toxin fractions.

Extraction and Isolation. The harvested *A. caterae* cells (110.83 g, wet weight) were extracted with 80% MeOH in H_2O (2 × 1.5 L) and MeOH (1 × 1.5 L). All extracts were combined and concentrated to dryness using a rotary evaporator at 40 °C. The dried extract (10.64 g) was partitioned between hexane (150 mL × 4) and MeOH (300 mL). Water was added to the MeOH layer to 50% followed by partitioning with CH_2Cl_2 (150 mL × 4). The MeOH/H_2O layer was dried and then partitioned between *n*-BuOH (300 mL) and H_2O (200 mL × 2). All *n*-BuOH layers were combined and dried at 37 °C in vacuo to provide a BuOH-soluble extract (337.4 mg). This extract was fractionated using a Sep-pak C_{18} column (20 g) using a stepped gradient of MeOH/H_2O elution. LC-MS analysis indicated a concentration of amphidinols in the 60% MeOH fraction. This was fractionated twice by HPLC, first using a semipreparative C_{18} column (Phenomenex Gemini; 10 × 250 mm, 5 μm) with a gradient mobile phase (50%−80% MeOH in H_2O over 23 min) and then using a C_1 column (Develosil TMS-UG-5; 4.6 × 250 mm) with an isocratic mobile phase (50% MeCN in H_2O containing 10 mM NH_4OAc) to yield purified AM17 (**1**; 1.3 mg).

Spent culture medium (supernatant) of *A. caterae* (190 L) was passed through a Bakerbond C_{18} column. After washing with a solution of 5% MeOH in H_2O to remove the inorganic salts, the column was eluted with MeOH/acetone (30 L; 2:1). The eluent was dried and partitioned between MeOH (200 mL) and hexanes (100 mL × 3). The MeOH layer was dried and then partitioned between *n*-BuOH (200 mL) and H_2O (150 mL × 2). The *n*-BuOH layer was dried in vacuo to provide an organic extract (408.1 mg), which was fractionated using a Sep-pak C_{18} column (20 g) and a stepped gradient of MeOH/H_2O. The 20% MeOH fraction was found to contain amphidinols by LC-MS analysis and was further separated using a Sephadex column, eluted with a mixture of hexanes/MeOH/*i*-PrOH (4:1:1) and a final wash with MeOH. The MeOH fraction containing AM17 (**1**) was fractionated twice by HPLC as described above to yield **1** (1.8 mg).

Amphidinol 17 (1): Pale yellow semisolid (3.1 mg); $[\alpha]^{25}_D$ −6.0 (*c* 0.10, MeOH); UV (MeOH) λ_{max} (log ε) 262 (3.03), 272 (3.14), 283 (3.03) nm; IR (film) ν_{max} 3563, 1640, 1563, 1540 cm^{-1}; ^{1}H and ^{13}C NMR Table 1; HRESIMS (+) *m*/*z* 1305.7004 (calcd for $C_{63}H_{110}O_{24}SNa$ 1305.7004; Δ = 0.0 ppm).

Incorporation of [2-^{13}C]Acetate. A mixture of [2-^{13}C]acetic acid (1.5 mL) and sodium [2-^{13}C]acetate (0.76 g) was dissolved in water and subjected to filtration at 0.22 μm. This labeled precursor was administered as a single addition to each of seven 10 L cultures of *A. carterae* (70 L; final concentration 0.5 mM) growing in medium and conditions as described above. At the time of the labeled precursor addition, a complete nutrient addition was added aseptically. One week after administration of precursor, the spent media were recovered by continuous centrifugation and preserved by addition of ∼1.0 mL of $CHCl_3$. Solid-phase extraction of the recovered media (70 L) was accomplished using a packed glass column containing Diaion HP-20 (Sigma-Aldrich) (10 × 24.5 cm; 1.5 kg) using a flow rate of 5 L/h for adsorption of organics to the resin. The column was washed with deionized water (5 L), and the bound materials were recovered by reverse elution with 50% aqueous acetone (3 L) and then 100% acetone (3 L) at 1.5 L/h. The resulting extract was then fractionated as described above, yielding 5 mg of labeled AM17 (**1**).

Acknowledgment. J.L.C.W. gratefully acknowledges funding support from NIH (5P41GM076300-01). This work was supported in part by MARBIONC (J.L.C.W. and C.T.). We thank Ms. J. Kelly for performing the hemolytic assay and Ms. A. Drummond for performing the antifungal assay.

Supporting Information Available: 1D and 2D NMR spectra for natural abundance **1** and labeled **1**; EPI spectrum of natural abundance

1; hemolytic assay EC_{50} curve for **1**. This material is available free of charge via the Internet at http://pubs.acs.org.

References and Notes

(1) Taylor, F. J. R. In *The Biology of Dinoflagellates*; Taylor, F. J. R., Ed.; Blackwell Scientific: Oxford, 1987; pp 723−731.
(2) Satake, M.; Murata, M.; Yasumoto, T.; Fujita, T.; Naoki, H. *J. Am. Chem. Soc.* **1991**, *113*, 9859–9861.
(3) Paul, G. K.; Matsumori, N.; Murata, M.; Tachibana, K. *Tetrahedron Lett.* **1995**, *36*, 6279–6282.
(4) Echigoya, R.; Rhodes, L.; Oshima, Y.; Satake, M. *Harmful Algae* **2005**, *4*, 383–389.
(5) Morsy, N.; Matsuoka, S.; Houdai, T.; Matsumori, N.; Adachi, S.; Murata, M.; Iwashita, T.; Fujita, T. *Tetrahedron* **2005**, *61*, 8606–8610.
(6) Morsy, N.; Houdai, T.; Matsuoka, S.; Matsumori, N.; Adachi, S.; Oishi, T.; Murata, M.; Iwashita, T.; Fujita, T. *Bioorg. Med. Chem.* **2006**, *14*, 6548–6554.
(7) Kubota, T.; Tsuda, M.; Doi, Y.; Takahashi, A.; Nakamichi, H.; Ishibashi, M.; Fukushi, E.; Kawabata, J.; Kobayashi, J.-i. *Tetrahedron* **1998**, *54*, 14455–14464.
(8) Huang, X.-C.; Zhao, D.; Guo, Y.-W.; Wu, H.-M.; Lin, L.-P.; Wang, Z.-H.; Ding, J.; Lin, Y.-S. *Bioorg. Med. Chem. Lett.* **2004**, *14*, 3117–3120.
(9) Washida, K.; Koyama, T.; Yamada, K.; Kita, M.; Uemura, D. *Tetrahedron Lett.* **2006**, *47*, 2521–2525.
(10) Huang, S.-J.; Kuo, C.-M.; Lin, Y.-C.; Chen, Y.-M.; Lu, C.-K. *Tetrahedron Lett.* **2009**, *50*, 2512–2515.
(11) Van Wagoner, R. M.; Deeds, J. R.; Satake, M.; Ribeiro, A. A.; Place, A. R.; Wright, J. L. C. *Tetrahedron Lett.* **2008**, *49*, 6457–6461.
(12) Paul, G. K.; Matsumori, N.; Konoki, K.; Murata, M.; Tachibana, K. *J. Mar. Biotechnol.* **1997**, *5*, 124–128.
(13) Morsy, N.; Houdai, T.; Konoki, K.; Matsumori, N.; Oishi, T.; Murata, M. *Bioorg. Med. Chem.* **2008**, *16*, 3084–3090.
(14) Morsy, N.; Konoki, K.; Houdai, T.; Matsumori, N.; Oishi, T.; Murata, M.; Aimoto, S. *Biochim. Biophys. Acta* **2008**, *1778*, 1453–1459.
(15) Chou, H.-N.; Shimizu, Y. *J. Am. Chem. Soc.* **1987**, *109*, 2184−2185.
(16) Lee, M. S.; Qin, G.; Nakanishi, K.; Zagorski, M. G. *J. Am. Chem. Soc.* **1989**, *111*, 6234–6241.
(17) Needham, J.; McLachlan, J. L.; Walter, J. A.; Wright, J. L. C. *J. Chem. Soc., Chem. Commun.* **1994**, 2599–2600.
(18) Needham, J.; Hu, T.; McLachlan, J. L.; Walter, J. A.; Wright, J. L. C. *J. Chem. Soc., Chem. Commun.* **1995**, 1623–1624.
(19) Wright, J. L. C.; Hu, T.; McLachlan, J. L.; Needham, J.; Walter, J. A. *J. Am. Chem. Soc.* **1996**, *118*, 8757–8758.
(20) MacPherson, G. R.; Burton, I. W.; LeBlanc, P.; Walter, J. A.; Wright, J. L. C. *J. Org. Chem.* **2003**, *68*, 1659–1664.
(21) Houdai, T.; Matsuoka, S.; Murata, M.; Satake, M.; Ota, S.; Oshima, Y.; Rhodes, L. L. *Tetrahedron* **2001**, *57*, 5551–5555.
(22) Murakami, M.; Okita, Y.; Matsuda, H.; Okino, T.; Yamaguchi, K. *Phytochemistry* **1998**, *48*, 85–88.
(23) Kobayashi, J.-i.; Kubota, T. *J. Nat. Prod.* **2007**, *70*, 451–460.
(24) MacKinnon, S. L.; Cembella, A. D.; Burton, I. W.; Lewis, N.; LeBlanc, P.; Walter, J. A. *J. Org. Chem.* **2006**, *71*, 8724–8731.
(25) McInnes, A. G.; Walter, J. A.; Wright, J. L. C.; Vining, L. C. In *Topics in Carbon-13 NMR Spectroscopy*; Levy, G., Ed.; Wiley: New York, 1976; pp 123−178.
(26) Xiang, L.; Kalaitzis, J. A.; Moore, B. S. *Proc. Natl. Acad. Sci. U.S.A.* **2004**, *101*, 15609–15614.
(27) Julien, B.; Tian, Z.-Q.; Reid, R.; Reeves, C. D. *Chem. Biol.* **2006**, *13*, 1277–1286.
(28) Eschbach, E.; Scharsack, J. P.; John, U.; Medlin, L. K. *J. Appl. Toxicol.* **2001**, *21*, 513–519.
(29) Keller, M.; Guillard, R. R. L. In *Toxic Dinoflagellates. Proceedings of the 3rd International Conference on Toxic Dinoflagellates*; Anderson, D. M., White, A. W., Baden, D. G., Eds.; Elsevier: New York, 1985; pp 113−116.

NP900616Q